An unexpected bonding interaction between d_{xy} and a_{1u} orbitals mediated by porphyrin deformation

Ru-Jen Cheng,* Yen-Ku Wang, Ping-Yu Chen, Ya-Ping Han and Chih-Ching Chang

Received (in Cambridge, UK) 15th October 2004, Accepted 26th November 2004
First published as an Advance Article on the web 21st January 2005
DOI: 10.1039/b416023c

Through density functional calculation and NMR spectroscopy, an unusual intermediate-spin electronic structure $(d_{xz}d_{yz})^3(d_{xy})^1(d_z2)^1$ has been assigned to the six-coordinate saddled $[Fe(OETPP)(THF)_2]^+$ complex instead of the corresponding ruffled $[Fe(TiPrP)(THF)_2]^+$ complex.

Ring deformation of porphyrin macrocycle has been noticed to be a novel mechanism to control the electronic structure of iron(III) porphyrins. While saddled deformation increases the stability of intermediate-spin state relative to the high-spin state for five-coordinate complexes,[1,2] ruffled deformation changes the electronic structure of six-coordinate low-spin complexes from $(d_{xy})^2(d_{xz}d_{yz})^3$ to $(d_{xz}d_{yz})^4(d_{xy})^1$.[3,4] All these electronic structure consequences could be rationalized through bonding characteristics mediated by porphyrin deformations.[5,6] Generally, deformation of porphyrin decreases the symmetry of the coordination sphere but increases the probabilities of bonding interactions between metal and macrocycle. The complementary nature of theoretical calculations and NMR spectroscopy of paramagnetic molecules makes possible a modern implementation for the bonding analyses of five- and six-coordinate high-spin iron(III) porphyrin complexes.[7] Bonding interaction between d_z2 and a_{2u}-type porphyrin molecular orbitals is symmetry-allowed for five-coordinate complexes with symmetry lower than C_{4v} but forbidden for six-coordinate complexes with symmetry higher than D_{2d}.

For low-spin six-coordinate ruffled metalloporphyrins, the well recognized symmetry-allowed bonding interaction between d_{xy} and a_{2u}[3] has been further confirmed by DFT-related theoretical calculation.[6] Another symmetry-controlled bonding interaction between d_x2-_y2 and a_{2u}, proposed to explain the antiferromagnetic coupling for the saddled $[Cu^{II}(OETPP)^{+\cdot}]^+$ complex,[8] has also been observed in the ZINDO-based molecular orbitals for Fe(OETPP)Cl.[5] So far, all these macrocycle deformation induced bonding interactions are related to a_{2u}-type porphyrin molecular orbital. For the a_{1u}-type porphyrin molecular orbital, similar symmetry consideration indicates the possibility of d_{xy}–a_{1u} and d_x2-_y2–a_{1u} orbital interactions in saddle- and ruffle-shaped complexes with D_{2d} symmetry (Table 1). However, to the best of our knowledge, none of these orbital interactions has been reported either experimentally or theoretically. It is our goal in this research to explore the possible existence of these novel interactions and the consequences of their corresponding electronic structures.

*rjcheng@mail.nchu.edu.tw

Saddled $[Fe(OETPP)(THF)_2]^+$ and ruffled $[Fe(TiPrP)(THF)_2]^+$ complexes have been characterized to be of nearly pure intermediate-spin (S = 3/2).[9] Furthermore, on the basis of the chemical shift of *meso*-carbon (Table 2) and the well known bonding interaction between d_{xy} and a_{2u} in ruffled complex, $[Fe(OETPP)(THF)_2]^+$ and $[Fe(TiPrP)(THF)_2]^+$ have been suggested to be of two different electronic structures $(d_{xy})^2(d_{xz}d_{yz})^2(d_z2)^1$ and $(d_{xz}d_{yz})^3(d_{xy})^1(d_z2)^1$, respectively.[10] It is our expectation that bonding capabilities of d_{xy} and d_x2-_y2 are crucial factors in tuning the stability of these two electronic structures. $[Fe(OETPP)(THF)_2]^+$ and $[Fe(TiPrP)(THF)_2]^+$ complexes with two different types of D_{2d} symmetry offer a good chance to check all a_{1u} related bonding interactions (Table 1).

Fig. 1 shows the molecular orbitals involving d_{xy} and d_x2-_y2 of saddle- and ruffle-shaped $[FeP(THF)_2]^+$ complexes resulted from spin-restricted ADF[11] calculations and displayed by MOLEKEL.[12] As expected, bonding interaction between d_{xy} and a_{2u} orbitals is clearly visible for the ruffled complex with orbital contributions of 64.2% d_{xy} and 31.8% a_{2u}. It's quite unexpected that, d_{xy} and a_{1u} can actually interact even more with orbital contributions of 62.6% d_{xy} and 34.5% a_{1u} for the saddled complex. On the other hand, while a_{2u} has bonding interaction with the metal d_x2-_y2 orbital in the saddled complex, the symmetry-allowed bonding interaction between d_x2-_y2 and a_{1u} orbitals is not visible at all in the ruffled complex. It is important to note that the percent contribution related mainly to the energy match of the fragment orbitals does not always parallel the strength of the bonding interaction. Other than the symmetry and the relative energy considerations, the effective orbital overlaps in space that are also shown in Fig. 1 have to be taken into account.[7] Contrary to previous expectation, both orbital contributions and

Table 1 Correlation table for the molecular orbitals of metalloporphyrin[a]

	D_{4h}	D_{2h}	D_{2d}[b]	C_{4v}	C_{2v}
Metal					
d_x2-_y2	b_{1g}	a_g	$b_2(b_1)$	b_1	$a_1(a_2)$
d_z2	a_{1g}	a_g	a_1	a_1	a_1
d_{xz}, d_{yz}	e_g	b_{2g}, b_{3g}	e	e	b_1, b_2
d_{xy}	b_{2g}	b_{1g}	$b_1(b_2)$	b_2	$a_2(a_1)$
Porphyrin					
LUMO	e_g	b_{2g}, b_{3g}	e	e	b_1, b_2
HOMO	a_{1u}	a_u	b_1	a_2	a_2
	a_{2u}	b_{1u}	b_2	a_1	a_1
HOMO-1	e_g	b_{2g}, b_{3g}	e	e	b_1, b_2

[a] Defining x and y axes as lying in the porphyrin plane along trans pyrrole nitrogens. [b] Symmetry representations for ruffle-shaped deformation are given in the parentheses.

Table 2 ^{1}H and ^{13}C NMR chemical shifts and [isotropic shifts][a] of bis-THF complexes taken in CD_2Cl_2 at 298 K[13]

Complexes	α-C	β-C	*meso*-C	*q*-C (*meso*-CH)	β-***H*** (β-C***H***$_2$)
OETPP	394 [244]	215 [67]	−269 [−389]	354 [214]	(11.1, 38.7) [9.0, 36.6]
TiPrP	−122 [−262]	22 [−111]	115 [−8]	(51) [17]	−35.5 [−44.8]

[a] $\delta_{iso} = \delta_{obs} - \delta_{dia}$, diamagnetic shifts were taken from the reference complexes $[Co(OETPP)(Im)_2]^+$ and $[Co(TiPrP)(Im)_2]^+$.

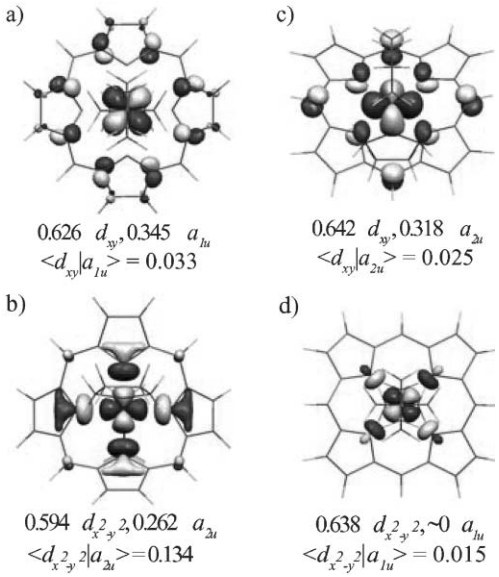

Fig. 1 Molecular orbitals based on spin-restricted calculations depict the bonding interactions between (a) d_{xy}–a_{1u} and (b) $d_{x^2-y^2}$–a_{2u} for saddled $[FeP(THF)_2]^+$, and the bonding interactions between (c) d_{xy}–a_{2u} and (d) $d_{x^2-y^2}$–a_{1u} for ruffled $[FeP(THF)_2]^+$. The corresponding orbital contributions and the effective orbital overlap in space are also shown under each molecular orbital.

orbital overlaps suggest that the bonding interaction between d_{xy} and a_{1u} orbitals in the saddled complex is stronger than bonding interaction between d_{xy} and a_{2u} orbitals in the ruffled complex.[10] While d_π-related bonding characteristics remain almost the same in these two complexes, the stronger bonding interaction and destabilization of d_{xy} in the saddled complex facilitate the formation of the unusual electronic structure $(d_{xz}d_{yz})^3(d_{xy})^1(d_z2)^1$.

Detailed analysis of the spin distribution on the macrocycle may disclose specific bonding interactions between iron and porphyrin,[7] and further confirm the electronic structure of the complex. The net spin populations and the nuclear spin populations on each symmetry-distinct atom type for $[Fe(OETPP)(THF)_2]^+$ and $[Fe(TiPrP)(THF)_2]^+$ with high-spin and two different intermediate-spin states from spin-unrestricted ADF calculations are summarized in Table 3. It is noteworthy that the spin populations are always more negative on *meso*-carbons but more positive on α,β-carbons for $[Fe(OETPP)(THF)_2]^+$. The most distinct feature is the spin populations for the unusual intermediate-spin state ^4E, which show opposite signs on *meso*- and α-carbons for $[Fe(OETPP)(THF)_2]^+$ and $[Fe(TiPrP)(THF)_2]^+$. This can be ascribed to the unpaired electron in d_{xy}. With the d_{xy}–a_{1u} bonding interaction in $[Fe(OETPP)(THF)_2]^+$, the unpaired electron from d_{xy} will delocalize to and result in positive spin densities at the α,β-carbons. Since a_{1u} orbital has nodes at the *meso* positions, spin polarization from neighboring α-carbons induces

Table 3 Net spin populations and [the nuclear spin populations] in the order of 10^{-4} on each symmetry-distinct atom type for bis-THF complexes from unrestricted DFT calculations

$[Fe(OETPP)(THF)_2]^+$	$^6A_2$[a]	$^4A_1$[a]	^4E[a]
meso-C	76 [3.8]	−232 [−26.6]	−384 [−52.2]
α-C	195 [46.5]	129 [3.3]	207 [42.6]
β-C	325 [75.2]	295 [31.7]	171 [17.8]
q-C	0 [9.6]	22 [7.7]	49 [25.4]
β-C***H***$_2$	11 [5.5]	11 [4.7]	0 [−0.1]
	8 [2.5]	5 [1.1]	7 [3.1]
$[Fe(TiPrP)(THF)_2]^+$	$^6A_2$[a]	$^4A_1$[a]	^4E[a]
meso-C	387 [52.3]	−109 [−11.7]	583 [90.0]
α-C	28 [52.5]	125 [−13.7]	−120 [−38.6]
β-C	207 [73.7]	216 [8.7]	40 [−5.7]
meso-C***H***	−28 [−11.7]	5 [1.0]	−36 [−14.9]
β-***H***	−2 [1.8]	−20 [−4.2]	−3 [−0.7]

[a] $^6A_2$ $(d_{xy})^1(d_{xz}d_{yz})^2(d_z2)^1(d_{x^2-y^2})^1$; $^4A_1$ $(d_{xy})^2(d_{xz}d_{yz})^2(d_z2)^1$; ^4E $(d_{xz}d_{yz})^3(d_{xy})^1(d_z2)^1$.

negative spin densities at the *meso*-carbons. The complementary nature of the orbital composition in a_{1u} and a_{2u} and the bonding interaction between d_{xy}–a_{2u} orbitals in $[Fe(TiPrP)(THF)_2]^+$ cause positive spin densities at the *meso*-carbons but negative spin densities at the α-carbons.

Qualitative comparison between the NMR data (Table 2)[13] and the spin populations (Table 3) might help to identify the major contribution from different electronic states. In the case of the $[Fe(TiPrP)(THF)_2]^+$ complex, the upfield shifts of α-, β-, *meso*-C and β-H are totally inconsistent with the spin populations of high-spin state $^6A_2$. Also the experimental isotropic shift –8 ppm of *meso*-C is not consistent with the very large positive spin population of ^4E, which in fact might be more close to the negative spin population of $^4A_1$ state. Accordingly, the correlation between the NMR data and the spin distributions of the $[Fe(TiPrP)(THF)_2]^+$ complex suggests the electronic structure of $^4A_1$ state with some minor contribution from ^4E. As to the $[Fe(OETPP)(THF)_2]^+$ complex, the unusually upfield isotropic shift –389 ppm of *meso*-C rules out the high-spin state but favors the intermediate-spin ^4E. And the facts that α-C is more downfield shifted than β-C and the *q*-C is also significantly downfield shifted further confirm the leading contribution of this unusual intermediate-spin state ^4E to the saddled $[Fe(OETPP)(THF)_2]^+$ complex.

In summary, both the bonding analyses and the spin distributions based on theoretical calculations and the NMR data from experiments strongly support our novel assignment of the unusual electronic structure $(d_{xz}d_{yz})^3(d_{xy})^1(d_z2)^1$ to the saddled $[Fe(OETPP)(THF)_2]^+$ complex. The unexpected symmetry-controlled bonding interaction of d_{xy}–a_{1u} *vs.* d_{xy}–a_{2u} makes the same electronic structure ^4E of saddled and ruffled complexes totally different in the spin distributions and the NMR consequences. Contrary to previous suggestions,[10] our conclusions

totally reverse the electronic structure assignments to the six-coordinate intermediate-spin $[Fe^{III}P(THF)_2]^+$ complexes with saddled and ruffled macrocycle deformation. As we all would expect, formation of the unusual electronic structure $(d_{xz}d_{yz})^3(d_{xy})^1(d_z2)^1$ *vs.* $(d_{xy})^2(d_{xz}d_{yz})^2(d_z2)^1$ depends mainly on the bonding nature of d_{xy} orbital. Stronger bonding interaction will destabilize d_{xy} relative to d_π orbitals and stabilize $(d_{xz}d_{yz})^3(d_{xy})^1(d_z2)^1$ electronic structure. On the basis of our bonding analyses, while ruffled deformation could facilitate bonding interaction between d_{xy}–a_{2u}, saddled distortion would induce even stronger bonding interaction between d_{xy}–a_{1u}. Therefore, it is reasonable for the saddled $[Fe(OETPP)(THF)_2]^+$ complex to have more contribution from $(d_{xz}d_{yz})^3(d_{xy})^1(d_z2)^1$ electronic structure. Ultimately, this is the only electronic structure that can explain the remarkable upfield shift of *meso*-C for $[Fe(OETPP)(THF)_2]^+$ complex. On the other hand, the significant upfield shift of *meso*-C for the ruffled $[Fe(TiPrP)(THF)_2]^+$ complex will never match the large positive spin population at *meso*-C of the $(d_{xz}d_{yz})^3(d_{xy})^1(d_z2)^1$ electronic structure. It is worth to mention at this point that *meso*-C chemical shift could be used as a powerful probe to determine the electronic configuration of the iron(III) porphyrin complexes[14] only if we know the bonding characteristics of the specific system. This report illustrates that lacking the knowledge of some crucial bonding interactions may result in quite different interpretation of the NMR data and the consequent electronic structures of paramagnetic complexes. And most of all, as the major part of our continuing research interest; once again we demonstrate that the symmetry-controlled bonding interaction may be a novel mechanism to fine-tune the versatile electronic structures of hemoproteins in nature.†

We are greatly indebted to Professor M. Nakamura for providing NMR data before publication. This work was supported by the National Center for High-Performance Computing and the National Science Council of Republic of China (NSC92-2113-M-005-013).

Ru-Jen Cheng,* Yen-Ku Wang, Ping-Yu Chen, Ya-Ping Han and Chih-Ching Chang
Department of Chemistry, National Chung-Hsing University, Taichung, Taiwan 402, Republic of China. E-mail: rjcheng@mail.nchu.edu.tw; Fax: 886-4-22862547; Tel: 886-4-22871190

Notes and references

† Computational Methods: Density functional calculations have been carried out for $[Fe^{III}P(THF)_2]^+$ (P = dianion of porphine with saddle- or ruffle-shaped deformation) complexes. Full geometry optimizations were done within D_{2d} and C_2 symmetry constraints for $[Fe(OETPP)(THF)_2]^+$ and $[Fe(TiPrP)(THF)_2]^+$ respectively with two planar THF rings perpendicular to each other along the concaves following trans pyrrole-nitrogens or *meso*-carbons. The optimized geometries with hydrogens replacing all substituents at *meso*- and pyrrole-β positions were used for the calculations for bonding analyses. Without the substituents both systems are of D_{2d} symmetry but of two different types of D_{2d} symmetry as shown in the correlation table (Table 1). All calculations reported in this paper are based on the Amsterdam density functional (ADF) program package characterized by the use of a density fitting procedure to obtain accurate Coulomb and exchange potentials in each SCF cycle, by accurate and efficient numerical integration of the effective one-electron Hamiltonian matrix elements, and by the possibility to freeze core orbitals.[15] The molecular orbitals were expanded in an uncontracted triple-ξ STO basis set, augmented with one 2p polarization function for hydrogen, one 3d function for carbon, nitrogen, and oxygen, and one 4p function for iron. The cores (Fe:1s–2p; C, N, O: 1s) have been kept frozen. The LSD exchange-correlation potential of Vosko-Wilk-Nusair (VWN) was used in all cases, along with the nonlocal Becke exchange correction[16] and nonlocal Perdew correlation correction.[17] Both spin-restricted and spin-unrestricted formalisms were used as specified for each calculation.

1 R.-J. Cheng, P.-Y. Chen, P.-R. Gau, C.-C. Chen and S.-M. Peng, *J. Am. Chem. Soc.*, 1997, **119**, 2563.
2 M. Nakamura, T. Ikeue, Y. Ohgo, M. Takahashi and M. Takeda, *Chem. Commun.*, 2002, 1198.
3 M. K. Safo, F. A. Walker, A. M. Raitsimring, W. P. Walters, D. P. Dolata, P. G. Debrunner and W. R. Scheidt, *J. Am. Chem. Soc.*, 1994, **116**, 7760.
4 M. Nakamura, T. Ikeue, H. Fujii and T. Yoshimura, *J. Am. Chem. Soc.*, 1997, **119**, 6284.
5 R.-J. Cheng and P.-Y. Chen, *Chem. Eur. J.*, 1999, **5**, 1708.
6 A. Ghosh, E. Gonzalez and T. Vangberg, *J. Phys. Chem. B*, 1999, **103**, 1363.
7 (*a*) A. Diefenbach, F. M. Bickelhaupt and G. Frenking, *J. Am. Chem. Soc.*, 2000, **122**, 6449; (*b*) R.-J. Cheng, P.-Y. Chen, T. Lovell, T. Liu, L. Noodleman and D. A. Case, *J. Am. Chem. Soc.*, 2003, **125**, 6774.
8 (*a*) Abbreviations used in this paper: P = dianion of porphin; TPP = dianion of *meso*-tetraphenylporphyrin; OETPP = dianion of octaethyltetraphenylporphyrin; TiPrP = dianion of *meso*-tetraisopropylporphyrin; (*b*) M. W. Renner, K. M. Barkigia, Y. Zhang, C. J. Medforth, K. M. Smith and J. Fajer, *J. Am. Chem. Soc.*, 1994, **116**, 8582.
9 T. Ikeue, T. Saitoh, T. Yamaguchi, Y. Ohgo, M. Nakamura, M. Takahashi and M. Takeda, *Chem. Commun.*, 2000, 1989.
10 T. Sakai, Y. Ohgo, T. Ikeue, M. Takahashi, M. Takeda and M. Nakamura, *J. Am. Chem. Soc.*, 2003, **125**, 13028.
11 E. J. Baerends and P. Ros, *Int. J. Quantum Chem.*, 1978, **S12**, 169.
12 P. F. Flukiger, H. P. Luthi, S. Portmann and J. Weber in '*MOLEKEL*', Manno (Switzerland), 2000–2002.
13 A. Hoshino, Y. Ohgo and M. Nakamura, *Inorg. Chem.*, 2004 submitted for publication.
14 M. Nakamura, A. Hoshino, A. Ikezaki and T. Ikeue, *Chem. Commun.*, 2003, 1862.
15 E. J. Baerends and P. Ros, *Int. J. Quantum Chem.*, 1978, **S12**, 169.
16 A. D. Becke, *Phys. Rev. A*, 1988, **38**, 3098.
17 J. P. Perdew, *Phys. Rev. B*, 1986, **33**, 8822.

